Proc. Indian natn. Sci. Acad., **60**, A, No. 3, 1994, pp. 513-533.

KALPATHI RAMAKRISHNA RAMANATHAN MEDAL LECTURE—1993

PREDICTION OF STORM SURGES IN THE BAY OF BENGAL

P K DAS

A/59, Kailash Colony, New Delhi-110048, India

(*Delivered* 31 *December* 1994)

The problem of storm surge prediction in the Bay of Bengal is reviewed in the context of the 'International Decade for Natural Disaster Reduction (IDNDR)'. Statistics are presented to show the damages caused by storm surges which come under the category of windstorms. The article describes recent developments in storm surge prediction by mathematical models. Starting with the basic formulation, the article discusses the forcing terms, namely, (*a*) the inverted barometer effect, (*b*) the wind stress and seabed friction and (*c*) the storm structure. A brief description is provided of statistical methods of predicting storm movement and trajectory. The lateral boundary conditions and the computational procedure for model integration are described, especially the inclusion of an irregular coast and a radiation condition for the open sea. The author has then presented results to indicate the performance of models for six major cyclones that have struck the eastern coast of India in the last two decades. In the last part of the paper, a short discussion is provided on (*a*) Tide-Surge interactions and (*b*) Interactions with wind driven waves. The results indicate that the former often tends to decrease the sealevel elevation, but the handicaps due to paucity of tide gauges hampers accurate model verification.

Key Words: Storm Surge Prediction; Bay of Bengal; Inverted Barometer Effect; Wind Stress; Seabed Friction; Storm Structure; Tide-Surge Interaction

Introduction

I feel honoured to speak on this occasion and would like to thank the Indian National Science Academy for inviting me to deliver the third Professor K R Ramanathan Commemoration Lecture. Professor Ramanathan was an outstanding scientist of our times. His work had a marked impact on all who had the good fortune to have known him. I was acquainted with his work towards the last phase of his career from 1948 to 1985, and I learnt a good deal from the way he studied large volumes of data with a keen analytical mind. He was always original in his approach and would never rest till he had extracted every bit of meaningful information from observations. His life showed us how we had an obligation to use data to support theoretical research.

I have chosen the topic of Storm Surges for this lecture because I was associated with this subject for a little over two decades. This is also apposite for this occasion because we are now in the midst of the International Decade for Natural Disaster Reduction (IDNDR). This emanates from a proposal by Pro-

fessor Frank Press, an eminent seismologist, before the United Nations in 1984. The proposal was accepted by the General Assembly of the United Nations in 1987 and the nineties were declared as the Decade for International Disaster Reduction.

Storm surges belong to the genre of natural disasters that are classified as "Windstorms". Table I provides an indication of the damages caused by natural hazards during the period 1900 to 1987.

Table I

Natural hazards (1900-1987)

Type	Damages (million U.S. dollars)	Fatal Casualties
Earthquakes	45,245	2,076,164
Floods	29,250	1,213,299
Windstorms (cyclones and surges)	14,100	686,849
Volcanoes	1,405	79,264
Landslides	720	21,904
Tsunamis	57	3,547
Total	90,777	4,081,027

(*Source*: *Disaster History to Present day Values*, Foreign Disaster Assistance, U.S. Aid Office, U.S.A.).

The geographical distribution of damages and casualties are shown in the following table:-

These tables suggest that the largest casualties occur over Asia and the southwestern parts of the Pacific. The damages are substantial. As shown in Table I, windstorms, which include storm surges, cause the largest damage after earthquakes and floods.

Tropical cyclones and storm surges are associated with very strong winds. The winds drive a large mass of water towards the coast leading to an inexor-

Table II

Human and material losses (1900-1987)

Region	Damages (million U.S. dollars)	Fatal casualties
Africa	6,945	21,651
Latin America and the Caribbean	22,422	284,369
Europe (including the former USSR)	38,747	286,487
Asia and S.W. Pacific	22,663	3,489,320
Total	90,777	4,081,027

(*Source*: As in Table I)

able rise in sealevel. This is the surge. It is a dangerously large ocean wave which is capable of crushing coastal structures and sweeping away all that comes before it. Large waves of this type are different from Tsunamis which are created by volcanic eruptions on the sea bed. With the exception of Tsunamis and tidal fluctuations, all ocean waves are created by winds exerting a stress over the underlying water.

Ocean waves travel in groups within a wide range of frequencies. A number of factors contribute to the development of waves. They include ocean currents, the depth of water and coastal topography. Waves which travel a long distance from the source of wind are known as swells. Swells often increase in amplitude when they encounter an ocean current coming from an opposite direction. Table III provides information on the frequency and periods of the principal oceanic waves.

Table III

Oceanic waves: frequencies and periods

Type	Frequency (Hz)	Period (hr)
1. Semi-diurnal tides		
(a) Lunar (M_2)	10^{-5}	12.4
(b) Solar (S_2)	10^{-5}	12.0
2. Storm surges	10^{-4}	3.0
3. Tsunamis	10^{-2}	3.0×10^{-2}
4. Swells and wind waves	10^{-1}	3×10^{-3}
5. Acoustic waves	10^{2}	3×10^{-6}

As we can see from this table, storm surges have a period comparable to semi-diurnal tides, especially the lunar semi-diurnal (M_2) tide whose amplitude is larger than the S_2 tide. Consequently, interactions between the surge and the M_2 tide are important for surge prediction. But, in shallow coastal regions, where the amplitude of the surge is comparable to the depth of the undisturbed sea, interactions between the surge, which is a long gravity wave and wind waves, which are short gravity waves, are also important. This is especially so for the northern sector of the Bay of Bengal and the Hoogly estuary. This region has a large tidal range. Considerable research is now in progress at different coastal stations on the nature of these interactions.

In this paper we will concentrate on surges generated in the Bay of Bengal, with a brief mention of the Arabian Sea. During the last two decades (1970-90) there were six major cyclones which have struck the coasts of India and Bangladesh. The landfall positions with approximate estimates of deaths are shown in Table IV.

It is interesting to note a gradual decline in the number of casualties on the Indian coast. This is an outcome of improvements in warning services. In this context, the Indian Space Research Organisation (ISRO), especially the INSAT series of Indian geostationary satellites, have made valuable contributions.

Table IV

Major tropical cyclones (1970-1991)

Year	Landfall	Country	Fatal casualties (Approx.)
1970	Chittagong	Bangladesh	300,000
1971	Paradip, Orissa	India	10,000
1977	Chirala, Andhra Pradesh	India	20,000
1982	Paradip, Orissa	India	250
1985	Hatia	Bangladesh	10,000
1990	Divi, Andhra Pradesh	India	950

Cyclone warnings are now disseminated on fast satellite links from an IMD Cyclone Warning Centre at Madras to all recipients. Wind and cloud data from the Indian satellites are also disseminated on the Global Telecommunication System (GTS) of World Weather Watch (WWW). World Weather Watch is a global system organised by the World Meteorological Organization (WMO) by which the major meteorological services of the world have agreed, voluntarily, to share their data and expertise through fast telecommunication links with other Member countries of WMO. This has helped to improve warning services against natural disasters.

Tropical cyclones occur more frequently in the Bay of Bengal compared to the Arabian Sea. The frequency of cyclones and surges is the highest in the premonsoon months of April and May and in the post-monsoon season from October to December. The Bay cyclones often enter the Bay of Bengal as remnants of tropical cyclones in the South China Sea. They intensify again on entering the Bay of Bengal. On some occasions they continue to move westwards and emerge into the Arabian Sea. Entering the Arabian Sea they intensify into a tropical cyclone and often recurve northwards towards Konkan and Gujarat. The coastal sector off the Rann and Kutch is vulnerable to large surges. As in the Hooghly estuary this region has also a large tidal range. A useful review of surges along the Indian coastline has been recently provided by Murty[1].

Early Studies on Surges

Work on storm surges began in India in the mid-sixties. Rao and Majumdar[2] used a nomogram designed by Sverdrup *et al.*[3] to estimate the amplitude of a surge from data on winds. Rao[4] later used this nomogram to delineate those sectors of the Indian coast that were most vulnerable to storm surges. A similar nomogram based on winds was used by Janardhan[5] to estimate the amplitude of surges off the island of Saugor at the northern end of the Bay of Bengal.

As surges are generated by cyclones the success of prediction depends on how well one can prognosticate the path of a cyclone, especially when it is ap-

proaching a coast. This is a difficult proposition, especially when a cyclone tends to recurve or change its course. Neumann and Mandal[6] devised a regression equation to predict the 72 hour displacement of a tropical cyclone by using the past locations of the storm centre, at intervals of 12 hours, as predictors. They found a linear combination of 4 predictors which explained 65% of the variance in the predicted location of the storm. The regression equation has not been tried extensively so far, but its application for predicting the landfall will be useful.

A different method was suggested by Chowdhury[7]. He considered a region bounded by two orthogonal planes to simulate the coasts of India and Bangladesh with an apex on the Hooghly estuary. In this region, he inserted a vortex with constant vorticity with its three images. The complex potential for his system provides a method of computing (*a*) the velocity components at different points in the region and (*b*) the path of the vortex. The method is simple and attractive and the results suggest that an accuracy of 20% can be achieved in predicting the landfall position. The assumption that the atmosphere is an ideal fluid with no viscosity is, however, a restriction.

More recently the path of a cyclone is predicted by numerical models. Very high resolution in space and time is required for this purpose. The present accuracy in predicting the landfall 24 hours ahead is between 150-200km for non-recurving storms. The accuracy is less for storms that recurve.

The classical picture of a cyclone is that of an axisymmetric Rankine vortex. The winds blow towards the storm centre in the lower troposphere and outwards away from the centre in the upper troposphere and the lower stratosphere. The inward moving winds conserve their angular momentum. This is the product of the tangential component (v) of the vector wind and the radial distance from the storm centre (r). As the product ($r \times v$) is conserved, increases with decreasing r, but the kinetic energy of a cyclonic vortex is finite, so v cannot increase indefinitely. There is a critical value of r beyond which the winds cannot penetrate inwards. This is the radius of maximum winds (R). The region $0 < r < R$ is the eye of the storm. It is a region of calm winds. Being unable to penetrate inwards beyond R, the winds spiral upwards and, eventually, join the outflow in the upper troposphere and the lower stratosphere. For most storms the value of R is about 50km, while the outer edge of the storm is located around 6 times R or 300km.

Recent observations suggest an asymmetry in the vortex circulation. The winds and the currents appear to be stronger towards the right rear quadrant of the vortex. This has been observed by research aircraft and the ocean buoys fitted with current meters in the United States. A striking example is provided by the observations recorded during the passage of hurricane Gilbert (1988) in the Gulf of Mexico. The intensification towards the right is believed to be an outcome of non-linearities in storm advection. Of considerable interest are inertial waves that are generated in the wake of a storm. These waves have a period around 1.5 days between 10°-20°N. Resonance between the phase of inertial waves and vertical baroclinic oscillations set up the storm could also cause a bias to the right of the storm track.

Multiple eyes (Willoughby[8]) have been recently observed. Observations indicate an inner eyewall that is surrounded by a concentric outer eyewall. The physical mechanism for multiple eyes is still unclear, but their appearance tends to become more prominent as the cyclone approaches land. They are believed to represent multiple zones of convection with more than one wind maxima. This is relevant for surge prediction as the wind stress determines the surge amplitude. Surge prediction models have not yet considered more than one wind maxima.

Surge Models

Models are built around the theory of shallow water waves. We assume that the depth of the sea is small compared to the lateral dimensions of the basin. In this case it is possible to neglect the vertical component of motion in comparison with the motion parallel to the free surface of water. This enables us to assume hydrostatic balance. In this approximation, the fluid is regarded as two dimensional with a depth averaged current, or transport vector ($\bar{V}$). Thus

$$\bar{V}=\int_h^{\zeta} V\mathrm{d}z, \qquad \ldots (3.1)$$

where ζ is the sealevel elevation above the undisturbed water depth $h(x, y)$. For convenience in notation, we will henceforth omit the overbar and regard V as the horizontal current or transport vector. The basic features of a model are expressed by the equations:

$$DV/Dt+f\boldsymbol{k}\times V+g\nabla(\zeta+p_a/g) + \alpha/H(\boldsymbol{\tau}^S-\boldsymbol{\tau}^B)+A_H\nabla^2 V=0, \qquad \ldots (3.2)$$

$$\partial\zeta/\partial t+\nabla\cdot(HV)=0 \qquad \ldots (3.3)$$

and

$$D/Dt=\partial/\partial t+V\cdot\nabla, \qquad \ldots (3.4)$$

where

$H=$ the total depth of water $(\zeta+h)$,
$p_a=$ atmospheric pressure,
$\rho=$ density of sea water,
$\alpha=$ specific volume,
$\boldsymbol{\tau}^S, \boldsymbol{\tau}^B=$ frictional stress at the free surface ($\boldsymbol{\tau}^S$) and the sea floor ($\boldsymbol{\tau}^B$),
$f=$ Coriolis parameter $(2\Omega\sin\phi)$,
$A_H=$ Coefficient of eddy viscosity

and $\boldsymbol{k}$ is the unit vector along the vertical axis of reference (Fig. 1).

Let z be a characteristic surge amplitude and T be a characteristic period. Then, the vertical velocity varies from zero on the sea bed to Z/T at the surface. From (3.3) we see that the horizontal current V is of the order $(Z/T\times L/H)$. Putting this in (3.4) we infer that as long as $Z/H<<1$, the nonlinear accelerations may be ignored in (3.2). Similarly, we find that the last term in (3.2)

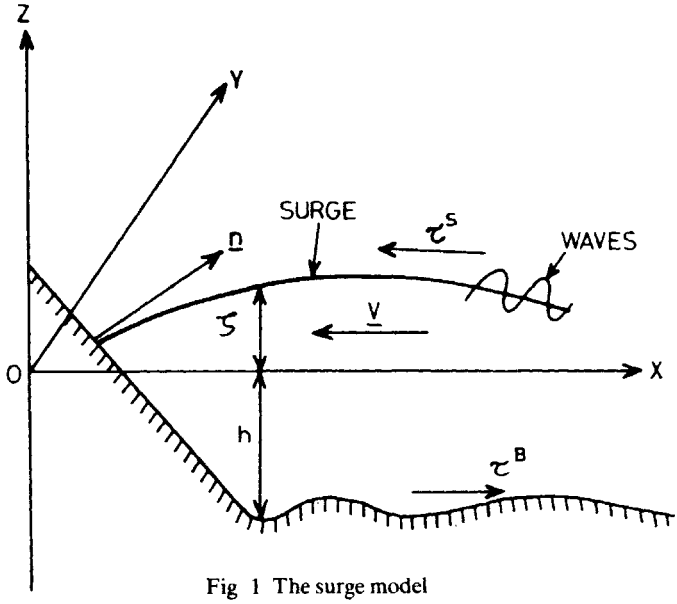

Fig 1 The surge model

containing the eddy viscosity may be ignored except in very shallow waters. More recent models have considered both these terms as well as the vertical profile of V, so that they are truly three-dimensional. More computer time is needed to work with three-dimensional models.

By elimination we find that the sealevel elevation (ζ) is expressed by the equation

$$[c^2\nabla^2-(\partial^2/\partial t^2+f^2)]\,\zeta_t=\frac{1}{\rho}(\nabla\cdot\boldsymbol{\tau})_t+f/\rho\,\boldsymbol{k}\cdot\nabla\times\boldsymbol{\tau}. \qquad \ldots (3.5)$$

This was derived by Lighthill[9]. The subscript t on the right is a time derivative and $\boldsymbol{k}$ is the unit vector in the vertical direction. The stress vector $\boldsymbol{\tau}$ is the difference between the wind stress and seabed friction. It is approximate measure of the wind stress, because seabed friction is small compared to the stress at the sea surface. The speed of gravity waves $(gH)^{1/2}$ is represented by c. If L represents a characteristic length and U^* is a friction velocity, then the non-dimensional equivalent of (3.5) is

$$[\nabla^2-F(\partial^2/\partial t^2+1)]\,\zeta_t=\lambda[(\nabla\cdot\boldsymbol{\tau})_t+\boldsymbol{k}\cdot\nabla\times\boldsymbol{\tau}] \qquad \ldots (3.6)$$

In the above equation the Froude Number (F) is defined by

$$F=f^2L^2/c^2 \qquad \ldots (3.7)$$

and λ the frictional coefficient, is given by

$$\lambda=-U_*^2/f^2LH. \qquad \ldots (3.8)$$

As we can see, the forcing terms are the time evolution of the stress divergence and the curl of the wind stress. Shay *et al.*[12] indicate that the curl is

the dominant term. Its magnitude is about 280×10^{-7} cm/s^2 in the region within $\pm R$, while the stress divergence is 50×10^{-7} cm/s^2.

Solutions of (3.5) and (3.6) may be derived in terms of a Green's function. This is expressed by a modified Bessel function (K_0). By taking Laplace transforms of ζ and τ and the inverse transform of the Green's function, it can be shown that in the early stages of the storm, the stress divergence is the only operative term. At a later stage the curl of the wind stress becomes more important. This was derived by Das[10] for a moving storm and by Das and Dube[11] for stationary storm. In the latter case, the spin-up time is $\sqrt{FR}$, where

$$R = [(X - X_0)^2 + (Y - Y_0)^2]^{1/2} \quad \ldots (3.9)$$

and X_0, Y_0 are the coordinates of the storm centre. Considering the following representative values:

$C = 1$ m/s, $\quad f = 10^{-5}$ s^{-1}

$L = 100$ km, $\quad F = 1.0$

the spin up time is about 12 hours for the region between $\pm R$. This is smaller than the period of inertial waves. Shay *et al.*[12] used a forced model to show how the divergence and the curl of the wind stress leads to a depression of the sea surface at the storm centre.

The Forcing Terms

Consider the forcing terms in (3.2)-(3.4) for surge prediction.

(*a*) *Atmospheric Pressure* (p_a)

Assuming that the air above the sea is in hydrostatic balance, it follows that a pressure deficit of 1mb will lead to a rise in sealevel by 1cm. This is the inverted barometer effect. The difference in atmospheric pressure between the centre of a storm and the undisturbed air at a large distance away from the storm centre provides an estimate of the rise in sealevel due to an inverted barometer. This is usually small in comparison with forcing by the wind stress. This, in turn, is determined by the winds generated by the gradient of atmospheric pressure.

(*b*) *With Stress and Seabed Friction*

The difference between the wind stress at the free surface and the seabed provides the main drive for the surge. The wind stress is expressed by the quadratic law

$$\tau = C_s \rho_a |U| U, \quad \ldots (3.10)$$

where U stands for the vector wind at 10m above the sea and ρ_a is the density of air. C_s is a surface drag coefficient. Most models use a constant value of 2.8×10^{-3} for C_s but C_s varies with wind speed and the stability of the atmosphere. Smith and Banke[13] for example, use the following expression to include the variation of C_s with wind speed

$$C_s = (0.63 + 0.066\, U_{10})^{-3} \quad \ldots (3.11)$$

Seabed friction is also expressed by the quadratic law

$$\boldsymbol{\tau}^B = C_B \rho |V| \, V, \qquad \ldots (3.12)$$

where C_B, the drag coefficient, is assigned a constant value of 2.5×10^{-3}. The height of the surge is sensitive to the choice of this constant, and the best value is obtained by experimentation for each region.

Early models used a steady Ekman Spiral over the seabed (Das[14]). This provides the following expression for the bottom stress

$$\boldsymbol{\tau}^B = \alpha V, \qquad \ldots (3.13)$$

where

$$\alpha = 0.035/\mathrm{h}^2 \, \mathrm{s}^{-1} \qquad \ldots (3.14)$$

The numerical constant (0.035) is obtained empirically by experimenting with different values of C_B. The bottom stress is inversely proportional to the square of the depth (h).

There are uncertainties in this method, because Ekman's Spiral assumes a constant eddy stress coefficient for the entire depth of the friction layer. It is also not clear how the time taken to generate a boundary layer over the bed of a shallow basin compares with the growth of a surge. But, Flierl and Robinson[15] omitted seabed friction in their model for the Bangladesh cyclone of 1970. They assumed that the depth of the friction layer would be small compared to the total depth of the fluid. The inclusion of seabed friction remains one of the main uncertainties in surge prediction. At low latitudes the depth of the Ekman layer is around 100m which is of the same order of magnitude as the depth of the sea.

Johns *et al.*[16] developed a closure (scheme from a balance equation for turbulent kinetic energy (E). A full three-dimensional model was used for this purpose. The balance equation for turbulent kinetic energy (E) equates the rate by which E is generated to (a) the rate of extraction of E from the mean flow, (b) the vertical redistribution of E according to a gradient transfer law and (c) the dissipation of E. An exchange coefficient (K) is used to evaluate (b) and (c). The exchange coefficient is determined by a similarity law, while the dissipation function is proportional to $E^{3/2}$. This closure scheme requires two additional boundary conditions to prevent the transfer of turbulent energy at the seabed and at the sea-surface. This form of closure has not been extensively used in storm surge models because Johns *et al.*[16] found there was little difference in the final output between a simpler two dimensional model with a quadratic law for bottom friction, and the multilevel model with a more sophisticated formulation for bottom stress. They tried both methods for the Andhra Pradesh cyclone of 1977.

(c) *Storm Structure and Circular Winds*

The structure of wind round a tropical cyclone may be inferred from the conservation of angular momentum.

Different models have been designed for this purpose. An early simple model by Das *et al.*[17] assumed the following pressure profile

$$p = 1010 - \Delta_p/(1+(r/R)^2), \quad \ldots (3.15)$$

where Δ_p is the pressure difference between the centre of the storm and the undisturbed atmosphere at a large distance away from the storm centre. The radial distance from the storm centre is r and R is the radius of the eye. Assuming a balance between the centrifugal force generated by the rotating winds and the pressure gradient force we find

$$V_m^2 = (13)^2 \times \Delta_p, \quad \ldots (3.16)$$

where V_m is in knots and Δ_p is expressed in millibars. The advantages of the method are its simplicity and the fact that Δ_p can be estimated from satellite data, but it does not specify the radius of the eye (R) explicitly.

Jelesnianski[18] suggested the following pattern for the wind speed

$$V = V_m(r/R)^{3/2}; \; r \leqslant R \quad \ldots (3.17)$$
$$= V_m(R/r)^{1/2}\, 1; \; r > R$$

Johns *et al.*[19] suggest a sharper cut-off for radial distances exceeding R. They suggest

$$V = V_m[\exp(R - R_1)/\alpha \times \exp(R_1 - r)/\beta], \quad \ldots (3.18)$$

where α, β and R_1 are length scales to determine the areal extent of the wind field. In practice it is difficult to determine these constants because wind data within a storm are difficult to come by. Numerical experimentation by Johns and his collaborators find that a proper representation of the wind field is crucial for surge prediction. They remark: "Wind speeds that are too great lead to a high surge response along the unrealistically long section of the coast". This is a relevant point because, unfortunately, we are unable to determine the lateral extent of a surge along the coast because of an inadequate network of tide gauges.

The above profiles provide for a maximum wind speed (V_m) at $r = R$, and a rapid fall thereafter. They also assume circular symmetry in the wind field, which is unrealistic. To get over this difficulty Jelesnianski and Taylor[20] introduced the expression

$$V = V_m \times 2\, rR/(r^2 + R^2) \quad \ldots (3.19)$$

This does introduce a certain amount of asymmetry, but these expressions do not tell us anything about wind direction. It is our expectation that future improvements in satellite and radar technology will provide better representation of the wind field within the cyclone, especially the bias towards the right of the storm track.

Lateral Boundary Conditions and Computational Procedures

Irregular Coasts

One of the difficulties that we encounter when we model a surge is to try and represent an irregular coast. Several devices have been tried of which only the principal ones are described here.

(i) *Staircase Models*

The coast is represented by small horizontal and vertical segments in the form of a staircase. This is shown in Fig. 2.

(ii) *Continuous Deformation*

It is often difficult to capture sharp changes in the curvature of a coast. Johns *et al.*[16] overcome this difficulty by introducing the transformation

$$\xi = [x - b_1(y)] \div b(y), \qquad \ldots (4.1)$$

where

$$b(y) = b_2(y) - b_1(y),$$

whence

$$\xi = 0;\ x = b_1(y) \qquad \ldots (4.2)$$

$$= 1;\ x = b_2(y)$$

The independent variables of a two-dimensional model are thus ξ, y and time (t). Dube *et al.*[21,22] have used this transformation extensively for their surge models.

(iii) *Conformation Transformation*

Wanstrath[23] converted a curved domain into a rectangle by a conformal transformation. This has not been used much for the Indian coast, but a brief account has been reported by Mahadevan[24].

It is not clear which is the best representation of an irregular coast. This view has been expressed that the staircase model tends to underestimate the peak surge by around 0.5m in regions of rapid change in coastal curvature, but this needs further study.

Coastal Boundary Conditions

The Indian models have used a reflective boundary condition at the coast. This assumes a vertical wall at the coast which makes the normal component of the transport vector ($\boldsymbol{V}$) vanish at the coast. We have (Fig. 1),

$$\boldsymbol{n} \cdot \boldsymbol{V} = 0, \qquad \ldots (4.3)$$

where $\boldsymbol{n}$ is the unit vector normal to the coast. As the coast is a sloping beach a more realistic boundary condition is

$$\partial/\partial t(\zeta + h) + \boldsymbol{V} \cdot \nabla(\zeta + h) = 0 \qquad \ldots (4.4)$$

The vector $\boldsymbol{V}$ now refers to the current at the coast. Unfortunately, this is not easy to apply because interactions between the surge and waves are most prominent at the coast. We will refer to this aspect later, but it is worth noting that (4.4) requires accurate data on coastal topography.

A radiation boundary condition is used at the open sea. This form of boundary condition prescribes outward propagation of energy from the domain affected by a surge, but prevents inward propagation of energy from the sea into the surge. Heaps[25] expressed this condition by

$$v + (g/h)^{1/2}\, \zeta = 0 \qquad \ldots (4.5)$$

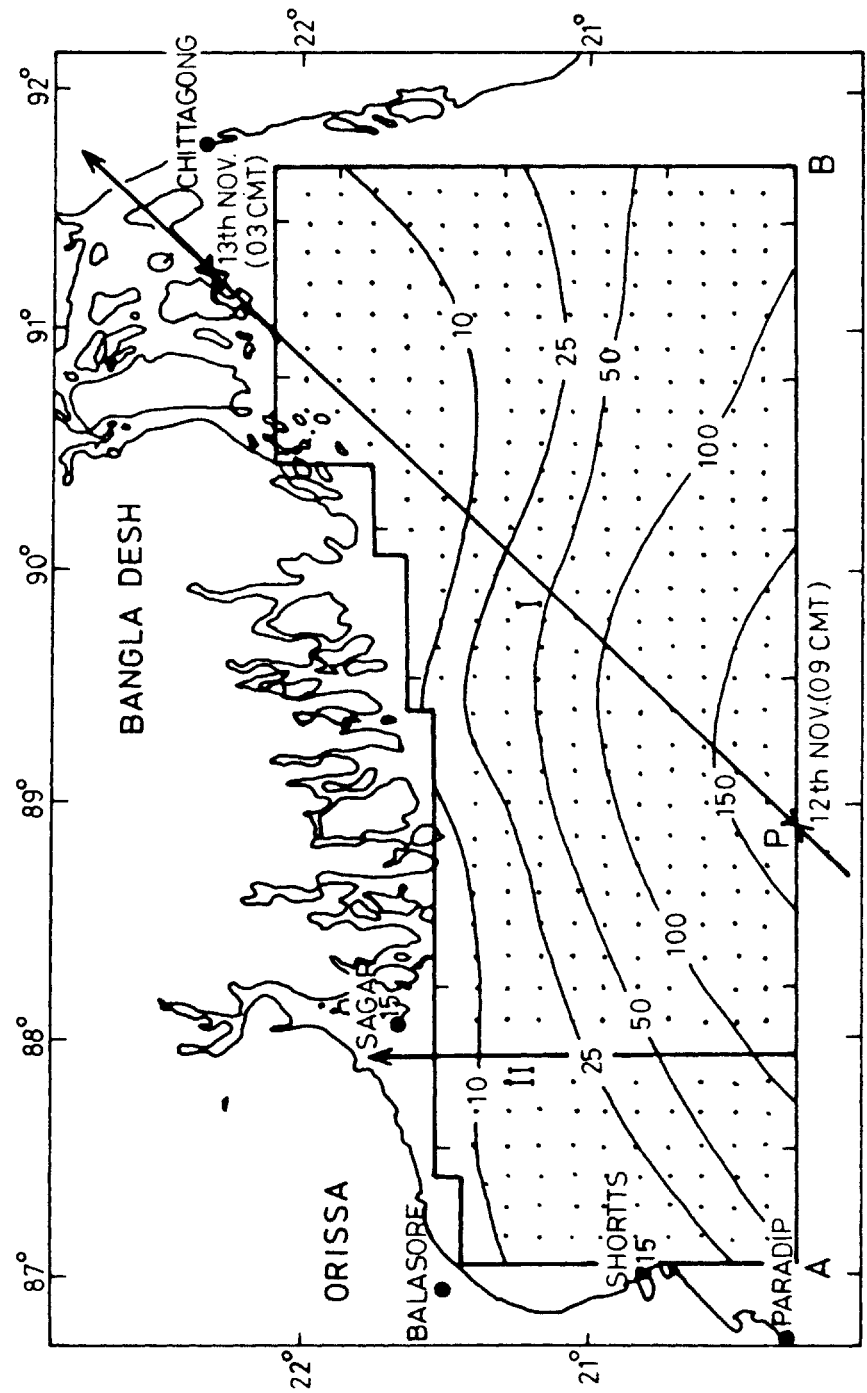

Fig 2 Grid for numerical integration by a Staircase model. I-Northeastward moving storm and II-Northward moving storm. Isopleths represent the depth of the sea in metres.

(a)

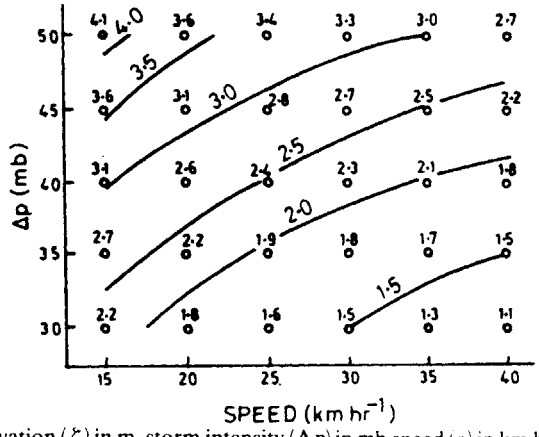

Sea level elevation (ζ) in m, storm intensity (Δp) in mb speed (c) in km h^{-1}. North-east

(b)

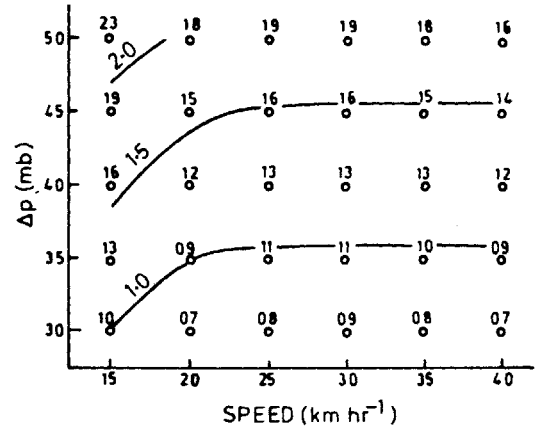

Sea level elevation (ζ) in m storm intensity (Δp) in mb and speed (c) in km hr^{-1}. North-ward

(c)

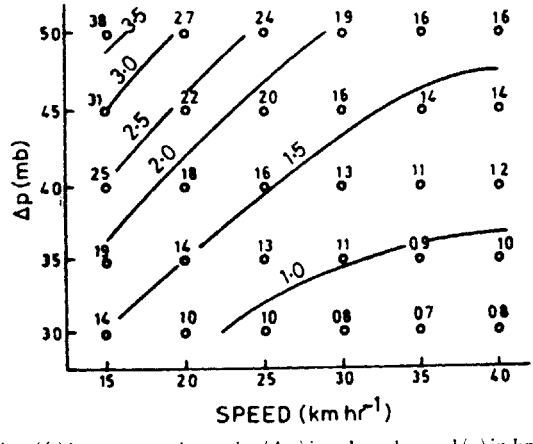

Sea level elevation (ζ) in m, storm intensity (Δp) in mb and speed (c) in km hr^{-1}. North-west

Note: Fig 3 Nomograms from model storms: (*a*) and (*b*) correspond to tracks I and II of FIg. 2(*c*)-III is for a storm moving northwestwards.

Computational Procedure

The finite difference analogues of (3.2) and (3.3) with a suitable representation of the forcing terms constitute the basic ingredients of a numerical model. Either cartesian or spherical coordinates may be used, but the independent variables are changed if stretched coordinates are used as by Johns *et al.* (*loc. cit*), or if a conformal transformation is made. The details of the latter have been explained in the review by Murty[1]. A staggered grid and a time stepping procedure is usually adopted. The staggered grid is designed to conserve the kinetic energy in the region of interest. This prevents the growth of nonlinear instability. A stability criterion, namely, the Courant-Friedrich-Levy criterion determines the size of time and space steps. We have

$$(gH)^{1/2}\,\Delta t/\Delta x < 1, \qquad \ldots (4.6)$$

where $(gH)^{1/2}$ is the speed of gravity waves and Δt, Δx are the time and space increments. For better resolution Das *et al.*[17] used a nested grid for the Orissa coast. This provides better resolution near the coast.

Results

It is difficult to compare model outputs with actual observations because of an inadequate network of tide gauges. On many occasions, no tide gauges exist at the point of landfall; consequently, the sealevel elevation is estimated from the observations at the nearest tide gauge.

Moreover, our understanding of interactions between the surge and wind driven waves near the coast is still unclear. Tide-surge interactions pose yet another problem. This depends on the phase of the astronomical tide. On some occasions the tide could depress the total sealevel instead of raising it (Johns *et al.*[26]).

The following tables indicate the principal features of the six storms mentioned in Table IV. The relevant data have been collected from the different publications by Murty, Dube *et al.*[28,29]. Table VI provides a comparison between the computed and observed peak surges with the addition of the tide.

Table V

Storm features

Date	Landfall	Central pressure (mb)	Pressure deficit (mb)	Max. Wind speed (km/hr.)
13 Nov 1970	Chittagong, Bangladesh	940	70	222
30 Oct 1971	Paradip, Orissa	960	40	167
19 Nov 1977	Chirala, Andhra Pradesh	909	101	250
3/4 June 1982	Paradip, Orissa	950	50	216
24 May 1985	Hatia, Bangladesh	975	21	120
9 May 1990	Divi, Andhra Pradesh	920	80	230

Table VI

Computed peak surge and observed surge + tide

Date	Computed peak surge (m)	Tide (m)	Observed Surge + Tide (m)
13 Nov 1970	4.1	1.8	6.0-9.0
30 Oct 1971	3.5	0.9	4.0-5.0
19 Nov 1977	5.0	0.3	5.0-6.0
3/4 June 1982	3.5	1.3	3.0
24 May 1985	2.0	1.7	4.5*
9 May 1990	4.3	0.3	4.0-5.0

(*) As reported by the Bangladesh Meteorological Department.

The above table shows reasonable agreement between the computed surge and the sealevel elevation (surge + tide), if we add the astronomical tide to the surge. But, as mentioned earlier, the model performance can be better assessed with a close network of tide gauges.

For real time prediction of the surge height model generated surges have been used to indicate the surge amplitude as a function of the pressure deficit (Δp) for different storm speed (c). Das *et al.*[17] computed the following expression

$$\zeta = a_0 \Delta p + a_1 (\Delta p)^2 + a_2 c, \qquad \ldots (5.1)$$

where a_0, a_1 and a_2 are constants. The constants were computed for storms having a landfall at the coastal sectors of (I) Bangladesh, (II) the Hooghly estuary and (III) the Orissa coast. Using numerical values of these constants, nomograms were prepared for these three sectors of the India-Bangladesh coast. The grid used for sectors I and II are shown in Fig. 2, while Fig. 3 gives the nomograms for I, II and III. The nomograms are for pressure deficits up to 50mb, but they could be extended to higher values of the pressure deficit by (5.1), if required. As we can see from these nomograms, the surge amplitudes approach a constant value for higher values of speed (c). This is because the sea has little time to respond to surges generated by fast moving storms.

A nomogram have been also prepared by Jelesnianski[27]. It is referred to as SPLASH (Special Programme for Listing Amplitudes of Surges from Hurricanes). Ghosh[28] used this for cyclones in the Bay of Bengal. SPLASH was later replaced by SLOSH which stands for "Sealevel over Land Surges from Hurricanes". These nomograms indicate the surge amplitude for different values of the eyewall radius (R).

These nomograms have their limitations because these are based on an idealised storm with a specific structure. The more recent trend is to compute the surge for each storm on a small computer located at a forecasting centre. In an innovative approach a standard computer programme for this purpose has been designed by Dube *et al.*[29]. This has an advantage because the meteor-

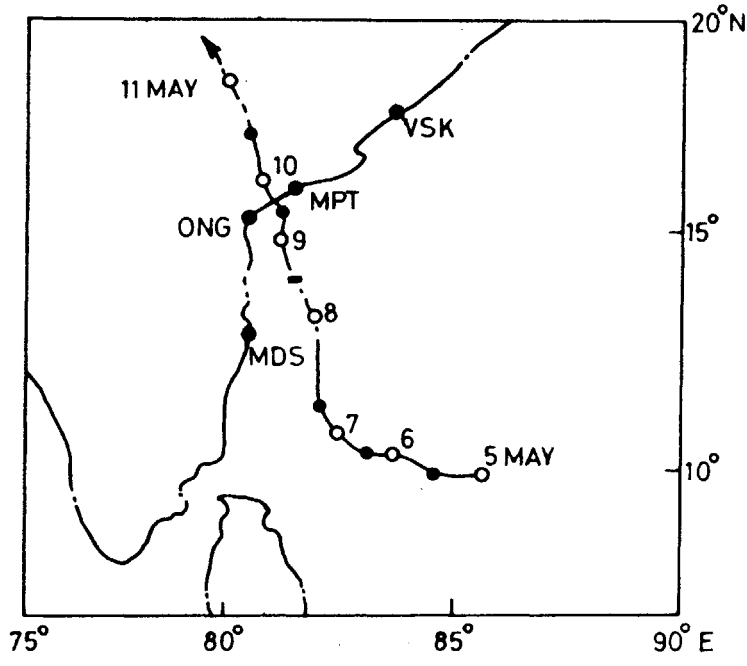

Fig 4 Storm track: Andhra Pradesh cyclone of 1990

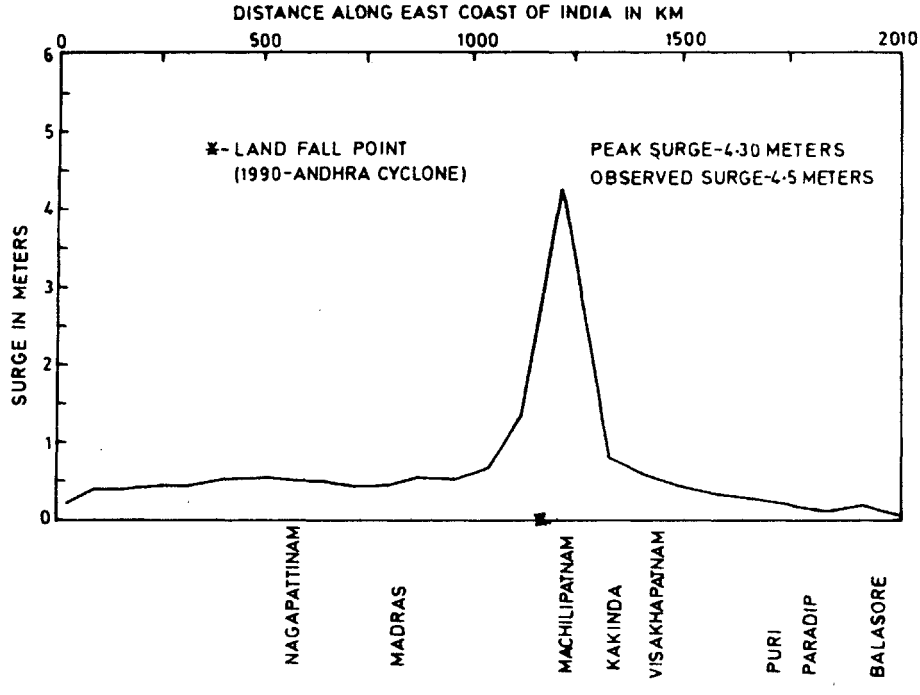

Fig 5 Andhra Pradesh cyclone of 1990: Surge profile computed on near real time[30].

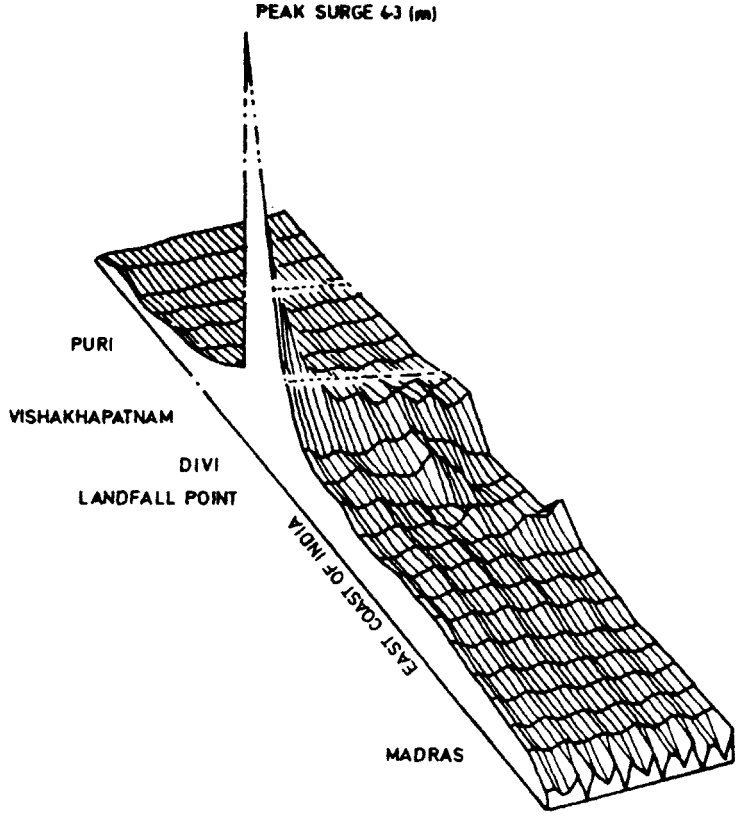

Fig 6 Three-dimensional surge profile[30].

ological input needed for surge prediction can be periodically updated with the inflow of data on fast telecommunication links. In Figs 4 & 5 we show the track of the Andhra Pradesh cyclone of 1990. Fig. 6 shows the three-dimensional profile of the peak surge at Divi evaluated from a computer. The computer also provides an indication of the surge profile if the landfall was either 100 km to the north, or to the south of the landfall anticipated by a forecaster. This is of considerable importance for real time prediction in an operational meteorological office. The details have been recently provided by Dube *et al.*[30].

Tide-Surge Interactions

These interactions are nonlinear so it is not strictly correct to superpose the astronomical tide on the surge. Das *et al.*[17] introduced the tide as an initial condition on the grid for the Bangladesh cyclone of 1970. This was done for different phases of the astronomical tide. It was found that simple superposition of the tide on the surge led to an overestimate of the total sealevel elevation. The difference could be as much as 0.8m at the time of high water. Tide-surge interactions could also lead to a difference in the computed time of max-

imum surge and the observed time of maximum sealevel elevation. The assumption of a constant speed of propagation for the storm could also lead to a discrepancy between the computed time of maximum surge and the observed highest sealevel rise. In this context, this points to the relevance of real time computation of a surge as by Dube *et al.* (*loc cit*).

A more detailed analysis was made by Johns *et al.* (*loc cit*). They also used a radiation boundary condition for tidal elevation along the open sea, but there are handicaps due to paucity of data. For example, the values of both ζ and v are not known with sufficient accuracy to use (4.5) with much confidence. An estimate of the tidal elevation ζ_T along the southern pen sea boundary would be

$$\zeta_T = a \sin [(2\pi t/T) + \phi] \qquad \ldots (6.1)$$

where a and ϕ represent the tidal amplitude and phase, while T is the period of the tide. If this was used in (4.5) we have

$$v + (g/h)^{1/2}\, \zeta = 2a\,(g/h)^{1/2} \sin[(2\pi t/T) + \phi]\,. \qquad \ldots (6.2)$$

As Johns *et al.* (*loc. cit*) point out, neither v nor a are known at the open boundary. Consequently, these parameters have to be determined by repeated experimentation to determine the values which give a realistic estimate.

An interesting part of the paper by Johns and his collaborators was the inclusion of river discharges at the head of the Bay of Bengal and the Orissa coast. An idealised river with a finite breadth and discharge was used to couple them to the surge model.

The general results of Johns *et al.* (*loc cit.*) again indicate a slight reduction in the peak surge amplitude, if the non-linear tide-surge interactions are considered. A simple superposition of the tide on the surge could thus lead to an overestimate. Another consequence of these interactions is to alter the time at which the peak elevation occurs. These results were observed for the Orissa cyclone of June 1982 and the Andhra Pradesh cyclone of November 1977 (Table I).

Wind Waves and Surge Interactions

Research on storm surges emphasises the importance of interactions between the surge and wind driven waves near the coast (Wolf *et al.*[31], Xioming Wu *et al.*[32]). Earlier it was felt that as waves and surges have disparate time scales interactions between them may not be important, but it is now seen that this cannot be ignored in shallow waters near the coast. Consequently, emphasis is being placed on developing suitable wave models which may be coupled to a surge model. Such models will be non-linear.

A wave is specified by its energy density spectrum $E(f, \theta, \boldsymbol{X}, t)$, where f and θ represent the frequency and direction of a wave at a location $\boldsymbol{X}$ and time t. The transformation of a wave as it approaches a coast proceeds in three stages. We have (*i*) a zone where the wave amplifies, (*ii*) a breaking zone and (*iii*) a run-up zone. The second zone is also referred to as a surf zone. It is here that the wave breaks and white-caps are generated. The flow parameters,

as a wave runs up the beach, measure its destructive properties. It is not always possible to divide the beach into the three distinct zones mentioned above, but the wave propagation is generally expressed by the equation

$$\partial E/\partial t + 1/2\, g\rho\, \nabla\cdot(C_g E) = S, \qquad \ldots (7.1)$$

where E is the wave energy density spectrum and C_g is the group velocity of waves in a specified frequency band and S is a source function which specifies the different sources and sinks of wave energy. The source function (S) is usually expressed by

$$S = S_{in} + S_{nl} + S_d \qquad \ldots (7.2)$$

where S_{in} is the energy input by the wind, S_{nl} is the redistribution of wave energy by nonlinear interactions and the last term (S_d) represents the dissipation of wave energy by wave breaking and seabed friction. The first term, namely, the input of energy has been expressed mathematically by Snyder *et al.*[33]. Their expression provides for an exponential growth of waves by the vector wind and the phase speed of waves. The latter is given by shallow water theory. A non-dimensional parameter which is of considerable importance in wave dynamics is the ratio

$$\omega^2 R/g\alpha^2,$$

where ω is the angular frequency of the wave ($\omega = 2\pi/T$), R is its characteristic height, α represents the slope of the beach, g is the gravitational constant and T is the wave period. This parameter could be incorporated in the first term of (7.2). The last term, namely, dissipation by seabed friction is expressed by a quadratic law as in the surge models described earlier.

There are different interpretations for the second term which represents non-linear interactions between waves of different frequencies, but a detailed discussion of this aspect will be outside the scope of this article.

Tides and waves modulate the storm induced surge despite the large difference in the time scales of tides and the surge on the one hand, and the waves on the other. This is because the cumulative effect of waves is to add, or extract momentum from the mean flow. Thus, the excess flux of momentum due to waves leads to a radiation stress (Longuet-Higgins and Stewart[34]). When waves enter a zone of shallow water without breaking, they add momentum to the mean flow. This is balanced by a decrease in the water level which is commonly referred to as a wave set down. Similarly, the radiation stress acting in the opposite direction extract momentum from the mean flow leading thereby to a wave set up. This occurs in the breaker zone and leads to an increase in water level. These effects provide additional forcing terms in the surge equations which have to be measured quantitatively.

This aspect of surge models is in an early stage in India at present, although work on the collection of wave statistics has started on selected areas of the Indian coastline. This will help us to predict the overall elevation due to the combined effects of a surge, the astronomical tide and wind-driven tides with better precision in the near future.

Summary and Conclusions

The main conclusions of this review of surge models in India may be summarised as follows:-

(i) Surges are long gravity waves associated with a tropical cyclone. Their periods are comparable with the lunar semi-diurnal tide.

(ii) Surges are responsible for long coastal inundation and damage to life and property. Their prediction is now possible on real time with computer oriented models.

(iii) The meteorological input for a model requires data on (*a*) the wind structure of a cyclone, (*b*) the radius of the eyewall and (*c*) a prediction of the cyclone's path and speed.

(iv) Coastal topography and bathymetry are needed for successful prediction, including more extensive data on the amplitude and phase of the semi-diurnal tides.

(v) A couple surge, tide and wave model will help to improve our understanding of coastal inundation. This requires more data on waves. An improvement in the network of wave recorders is desirable.

Acknowledgements

I am indebted to Professors P C Sinha and S K Dube at the Centre for Atmospheric Sciences, Indian Institute of Technology, New Delhi, and to Dr G S Mandal and Mr M C Pant of the Meteorological Department of India for their kind assistance in preparing this article.

References

1 T S Murty *Storm Surges, Meteorological Ocean tides*, Inst. Ocean Studies, Dept. of Fisheries and Oceans, Ottawa, Canada (1984) 897pp
2 N S B Rao and S Mazumdar A technique for forecasting storm waves, *Indian J Met Geophys* **17**(3) (1966) 333-346
3 H U Sverdrup, M W Johnson and R H Flemins *The Oceans, Their Physics, Chemistry and General Biology* Prentice Hall, New York (1946) 1060 pp
4 N S B Rao On some aspects of local and tropical storms in the Indian area, *Ph.D. Thesis*, Univ Jadavpur (1968) 262pp
5 S Janardhan *Indian J Met Geophys* **18** (1967) 205-212
6 C J Neumann and G S Mandal *Indian J Met Geophys* **28**(3) 487-500
7 A M Chowdhury *Nucl Sci Appl Ser* **AII** (1978) 1-7
8 H E Willoughby *J atmos Sci USA* **47** (1990) No. 2, 243-264
9 M J Lighthill *Phil Trans R Soc London* **A265** (1969) 49-93
10 P K Das *Proc Indian Acad Sci (Engn Sci) Bangalore* **4** (1981) 3, 269-276
11 P K Das and A P Dube *Proc Indian Acad Sci Bangalore* (1989) 205-212
12 Lynn K Shay, S W Chang and R L Elsberry *J phys Oceanogr USA* **20** (1990) 1405-1424
13 S D Smith and E G Banke *Q J R met Soc* **101** (1975) 665-673
14 P K Das *Nature (London)* **239** (1979) 211-213
15 G Flierl and A R Robinson *Nature (London)* **239** (1979) 213-215
16 B Johns, P C Sinha, S K Dube, U C Mohanty and A D Rao *Q J R met Soc* **109** (1983) 211-224
17 P K Das, M C Sinha and V Balasubramanyam *Q J R met Soc* **100** (1974) 437-449
18 C P Jelesnianski *Mon Wealth Rev U S Dept Agric* **93** (1965) 343-358

19 B Johns, A D Rao, S K Dube and P C Sinha *Phil Trans R Soc London* **A313** (1985) 507-535
20 C P Jelenianski and A D Taylor *NOAA Tech Mem ERL-WMPO* **3** (1973) NOAA Washington D C 33pp
21 S K Dube, P C Sinha and A D Rao *Mausam* **32** (1981) 315-320
22 —— *Mausam* (1982) 445-450
23 J J Wanstrath *Storm Surge Simulation in Transformed Coordinates, Vol II: Program Documentation Tech Rep No.* 76-3, US Army Corps of Engineers V A (1976) 176pp
24 R Mahadevan *Proc Math Modelling C-MMACS Bangalore* (1991) 13pp
25 N A Heaps *Phil Trans R Soc London* **A265** (1969) 93-137
26 B Johns, A D Rao, S K Dube and P C Sinha *Phil Trans R Soc London* **313** (1985) 507-535
27 C P Jelesnianski *SPLASH NOAA Tech Mem* **NWS-TDL-52** NOAA Washington (1974) 50pp
28 S K Ghosh *Indian J Met Hydrol & Geophys* **28**(2) (1977) 157-168
29 S K Dube *Proc ICSU/WMO Sem Tropical Cyclone Disasters* (1992) Beijing China
30 S K Dube, A D Rao, P C Sinha and P Chittibabu *Proc Indian natn Sci Acad (Phys Sci)* **60A**(1) (1994) 157-170
31 J Wolf, K P Hubbert and R A Flather *Proudman Oceanographic Lab Rep. No.* 1 **109**pp Bidston Obsy UK
32 Xioming Wu and R A Flather *Examples of the Interaction of Waves with Tides and Surges Proudman Ocean Lab UK* (1992) (*Under publication*)
33 R L Snyder, F W Dobson, J A Elliot and R B Long *J Fluid Mech* **102** (1981) 1-59
34 M S Longuet Higgins and R W Stewart *Deep Sea Res* **11A** (1964) 529-562